Joint Statistics between Velocity and Reactive Scalar in a Turbulent Liquid Jet with a Chemical Reaction

Tomoaki Watanabe, Yasuhiko Sakai, Kouji Nagata and Osamu Terashima

Department of Mechanical Science and Engineering, Nagoya University, Nagoya 464-8603, Japan

E-mail: watanabe.tomoaki@c.nagoya-u.jp

This version is free to view and download for private research and study only.
https://doi.org/10.1088/0031-8949/2013/T155/014039

Abstract. Joint statistics between velocity and concentration of reactive species are experimentally investigated in a planar liquid jet with a second-order chemical reaction A + B $\rightarrow$ R. Reactant species A and B are premixed in a jet flow and a main flow, respectively. An optical fiber probe based on light absorption spectrometry is used to measure the instantaneous concentrations of reactive species. The streamwise velocity and the concentrations of reactive species are simultaneously measured by combining the optical fiber probe with I-type hot-film anemometry, and we investigate the influences of the chemical reaction on correlation coefficients, joint probability density functions and cospectra of u and γ_i, where u is the streamwise velocity fluctuation and γ_i is the concentration fluctuation of species i. The results show that the absolute value of the correlation coefficient between u and γ_B becomes small owing to the chemical reaction whereas that between u and γ_A becomes large on the jet centreline. It is also shown that the influence of the chemical reaction on the cospectrum of u and γ_i in the upstream region and near the jet centreline is different from that in the downstream region and the outer edge of the flow.

PACS numbers: 47.27.tb, 47.51.+a, 47.70.Fw

Submitted to: *Phys. Scr.*

1. Introduction

Turbulent mixing with chemical reactions is commonly seen in industrial fields. For example, predictions of combustion efficiency and pollutant dispersion are important in engineering. From a practical viewpoint, turbulent models and models for

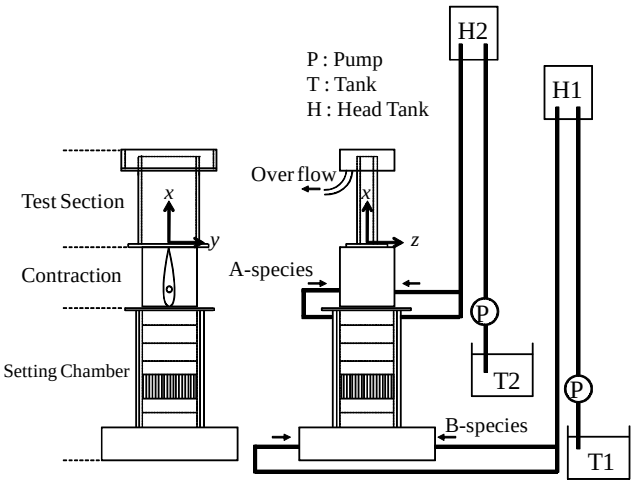

Figure 1. Experimental apparatus.

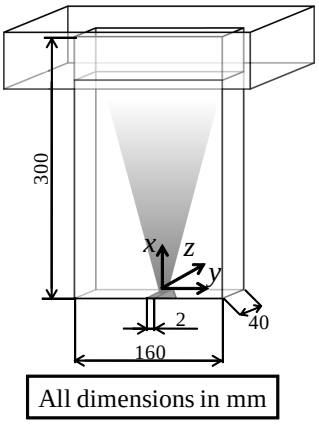

Figure 2. Test section.

chemical reaction rates[1][2] are often used to predict turbulent flows with chemical reactions. Therefore, it is important to verify these models for turbulent reacting flows. For verification of models for turbulent reacting flows, instantaneous velocity and instantaneous concentrations of multiple reactive species should be simultaneously measured by experiments because some models need joint statistics of concentration and velocity.

In the gas phase, simultaneous measurements of velocity and concentration of reactive species have been made for a scalar mixing layer in grid turbulence[3], a plume in grid turbulence[4] and a line source in grid turbulence[5]. By contrast, in the liquid phase, it is difficult to measure concentration of reactive species because the Batchelor scale, which is the smallest scale of scalar fluctuation, is very small owing to the high Schmidt number. Measurements of instantaneous concentration of reactive species have been made in grid turbulence[6][7][8], a planar jet[9] and a confined coaxial jet[10]. However, because simultaneous measurements of velocity and concentration of reactive species have been carried out by few researchers[11], there is little information available on the joint statistics between velocity and concentration in a turbulent reactive flow.

In this study, we perform simultaneous measurements of streamwise velocity and concentrations of reactive species in a planar liquid jet by combining I-type hot-film anemometry with an optical fiber probe based on light absorption spectrometry[12][13], and we investigate the influences of the chemical reaction on correlation coefficients, joint probability density functions and cospectra of streamwise velocity fluctuation u and concentration fluctuation of reactive species, γ_i.

2. Experimental Setup

The experimental apparatus is shown in Fig. 1. Solutions for the main flow and the jet flow are prepared in Tank 1 and Tank 2, respectively. To keep the flow rates of the

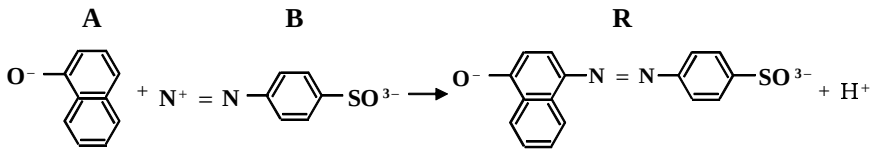

Figure 3. Details of the chemical reaction.

main flow and the jet flow at a jet exit constant, the main flow and the jet flow are supplied to the test section through Head Tank 1 and Head Tank 2, respectively. The streamwise mean velocity of the main flow is $U_M = 0.073$ m/s and the mean velocity of the jet flow at the jet exit is $U_J = 1.29$ m/s. Figure 2 shows the details of the test section. The cross section of the test section is rectangular with a width of 160 mm and a length of 40 mm, and the height of the test section is 300 mm. The width of the rectangular slit through which the jet flow is ejected is $d = 2$ mm. The Reynolds number, $Re = (U_J - U_M)d/\nu$, is 2 200, where ν is the kinematic viscosity. x and y are the streamwise direction and the cross-stream direction, respectively, with z completing the coordinate system. The origin of the coordinate system is located at the medium point of the slit.

The chemical reaction investigated in this study is a second-order reaction given by

$$\mathrm{A} + \mathrm{B} \rightarrow \mathrm{R}. \tag{1}$$

The reactants are 1-naphthol (A) and diazotized sulphanilic acid (B). The product is 4-(4′-sulphophenylazo)-1-naphthol (R), briefly referred to as monoazo dyestuff. Figure 3 shows the details of the chemical reaction. This chemical reaction is the first reaction of a set of series–parallel reactions that have been investigated thoroughly[14]. The reaction rate constant of the reaction given by Eq. (1) is $k = 12\,000$ m^3/(mol· s) under the present experimental condition. An aqueous solution of species B entered into the test section as the main stream and an aqueous solution of species A is issued into the main stream as a planar jet. The initial concentrations of species A and B, denoted by Γ_{A0} and Γ_{B0}, are 0.4 and 0.2 mol/m^3, respectively. Hence, the Damköhler number, $Da = k(\Gamma_{A0} + \Gamma_{B0})d/(U_J - U_M)$, is 11.8. The pH is kept constant by adding buffer salts (sodium carbonate and sodium hydrogen carbonate) into the jet flow because of the pH dependency of the above chemical reaction. To measure the concentrations of reactant species by using the mass conservation law, blue dyestuff (species C: Acid Blue 9) is added into the jet flow. The initial concentration of species C is $\Gamma_{C0} = 0.1$ kg/m^3. We have confirmed that species C is not affected by the above chemical reaction. Therefore, the concentration of species C can be considered as a conserved scalar, which is independent of the chemical reaction. Since species R and C are dyestuff and have light absorption characteristics, we can use light absorption spectrometry to measure the instantaneous concentrations of these two species.

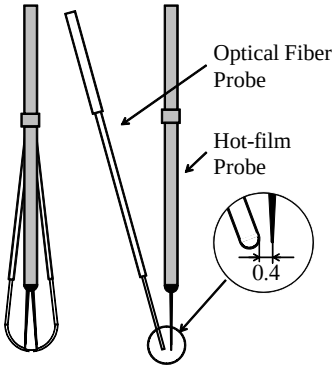

Figure 4. The combined probe.

3. Measurement Method

The concentrations of absorptive species R and C are measured by an optical fiber probe[13][16] based on light absorption spectrometry. If one assumes that light of wavelength λ passes through a solution of one absorptive species i, the light absorption spectrum denoted by $\tilde{P}(\lambda)$ is defined as follows:

$$\tilde{P}(\lambda) = -\ln \frac{\tilde{I}(\lambda)}{I_0(\lambda)}, \tag{2}$$

where $I_0(\lambda)$ is the intensity of incident light and $\tilde{I}(\lambda)$ is the instantaneous intensity of transmitted light. The tilde ($\tilde{}$) is used throughout to denote the instantaneous value. From Beer's absorption law, we can write $\tilde{P}(\lambda)$ as

$$\tilde{P}(\lambda) = k_i(\lambda)\tilde{\Gamma}_i, \tag{3}$$

where $\tilde{\Gamma}_i$ is the instantaneous concentration of absorptive species i and $k_i(\lambda)$, the light absorption coefficient, is given by $k_i(\lambda) = \alpha_i(\lambda)l$, where $\alpha_i(\lambda)$ depends on the absorptive characteristics of species i.

When a solution contains multiple absorptive species, $\tilde{P}(\lambda)$ is equal to the sum of each $\tilde{P}(\lambda)$ for the solution of one absorptive species. In this study, the flow contains two absorptive species R and C. Hence, for light of wavelength λ_n, $\tilde{P}(\lambda_n)$ is written as

$$\tilde{P}(\lambda_n) = -\ln\frac{\tilde{I}(\lambda_n)}{I_0(\lambda_n)} = k_R(\lambda_n)\tilde{\Gamma}_R + k_C(\lambda_n)\tilde{\Gamma}_C. \tag{4}$$

Here, $k_R(\lambda_n)$ and $k_C(\lambda_n)$ for the solution of two absorptive species R and C are the same as $k_R(\lambda_n)$ and $k_C(\lambda_n)$ for the solution that involves one species R or C. Hence, we can obtain the instantaneous concentrations of two absorptive species R and C from $\tilde{P}(\lambda)$ for two wavelengths measured by the optical fiber probe and $k_R(\lambda_n)$ and $k_C(\lambda_n)$ investigated previously.

The concentrations of species A and B cannot be measured by light absorption spectrometry because these two species do not have absorptive characteristics. However, the instantaneous concentrations of species A and B can be determined by adopting

conserved scalar theory[3]. According to conserved scalar theory, the instantaneous concentrations of species A and B are given by

$$\tilde{\Gamma}_A = \tilde{\xi}\Gamma_{A0} - \tilde{\Gamma}_R, \tag{5}$$

$$\tilde{\Gamma}_B = (1-\tilde{\xi})\Gamma_{B0} - \tilde{\Gamma}_R, \tag{6}$$

where $\tilde{\xi}$ is called the mixture fraction. In this study, the mixture fraction is defined by the concentration of nonreactive species C normalized by Γ_{C0}:

$$\tilde{\xi} = \tilde{\Gamma}_C/\Gamma_{C0}. \tag{7}$$

If $\tilde{\Gamma}_R$ and $\tilde{\xi}$ are known, we can calculate the instantaneous concentrations of species A and B from the mass conservation law written as Eqs. (5) and (6).

From Eqs. (5) and (6), the mass conservation law is rewritten as follows:

$$\frac{\tilde{\Gamma}_A}{\Gamma_{A0}} + \frac{\tilde{\Gamma}_B}{\Gamma_{B0}} + \frac{\tilde{\Gamma}_R}{\Gamma_{R0}} = 1, \tag{8}$$

where Γ_{R0} is defined as

$$\Gamma_{R0} = \frac{\Gamma_{A0}\Gamma_{B0}}{\Gamma_{A0}+\Gamma_{B0}}. \tag{9}$$

Under the present experimental conditions, $\Gamma_{R0} = 0.133$ mol/m^3.

The frozen limit corresponding to the limiting case of no reaction ($k \to 0$) is derived as follows:

$$\lim_{k\to 0} \tilde{\Gamma}_A = \tilde{\Gamma}_A^0 = \tilde{\xi}\Gamma_{A0}, \tag{10}$$

$$\lim_{k\to 0} \tilde{\Gamma}_B = \tilde{\Gamma}_B^0 = (1-\tilde{\xi})\Gamma_{B0}, \tag{11}$$

$$\lim_{k\to 0} \tilde{\Gamma}_R = \tilde{\Gamma}_R^0 = 0. \tag{12}$$

Furthermore, we can derive the equilibrium limit corresponding to the limiting case of the fast chemical reaction ($k \to \infty$) as follows;

$$\lim_{k\to\infty} \tilde{\Gamma}_A = \tilde{\Gamma}_A^\infty = (\Gamma_{A0}+\Gamma_{B0})(\tilde{\xi}-\xi_S)H(\tilde{\xi}-\xi_S), \tag{13}$$

$$\lim_{k\to\infty} \tilde{\Gamma}_B = \tilde{\Gamma}_B^\infty = (\Gamma_{A0}+\Gamma_{B0})(\xi_S-\tilde{\xi})H(\xi_S-\tilde{\xi}), \tag{14}$$

$$\lim_{k\to\infty} \tilde{\Gamma}_R = \tilde{\Gamma}_R^\infty = \Gamma_{B0}(1-\tilde{\xi})H(\tilde{\xi}-\xi_S) + \Gamma_{A0}\tilde{\xi}H(\xi_S-\tilde{\xi}). \tag{15}$$

Here, $H(z)$ is the Heaviside step function, and is equal to 0 for $z \leq 0$ or 1 for $z > 0$. ξ_S is the stoichiometric ratio of the reactant species in mixture, and is given by $\xi_S = \Gamma_{B0}/(\Gamma_{A0}+\Gamma_{B0})$. Under the present experimental conditions, $\xi_S = 0.333$. The experimental results are compared with the results for the frozen limit and the equilibrium limit.

In this study, we simultaneously measured the streamwise velocity and the concentrations of species R and C by the combined probe consisting of the optical fiber probe and an I-type hot-film probe. The details of the combined probe are shown in Fig. 4. The distance between the two probes is 0.4 mm. It has been verified that the simultaneous measurements of velocity and concentration can be accurately conducted by this combined probe in the jet flow[16].

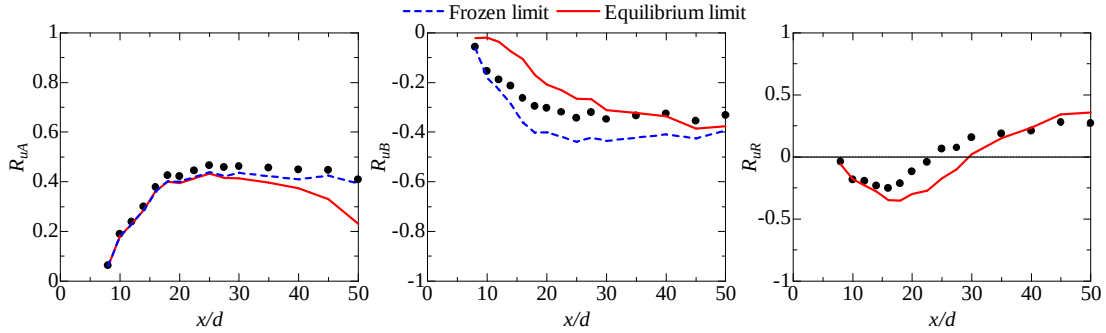

Figure 5. The streamwise evolution of the correlation coefficients of the velocity fluctuation and the concentration fluctuation.

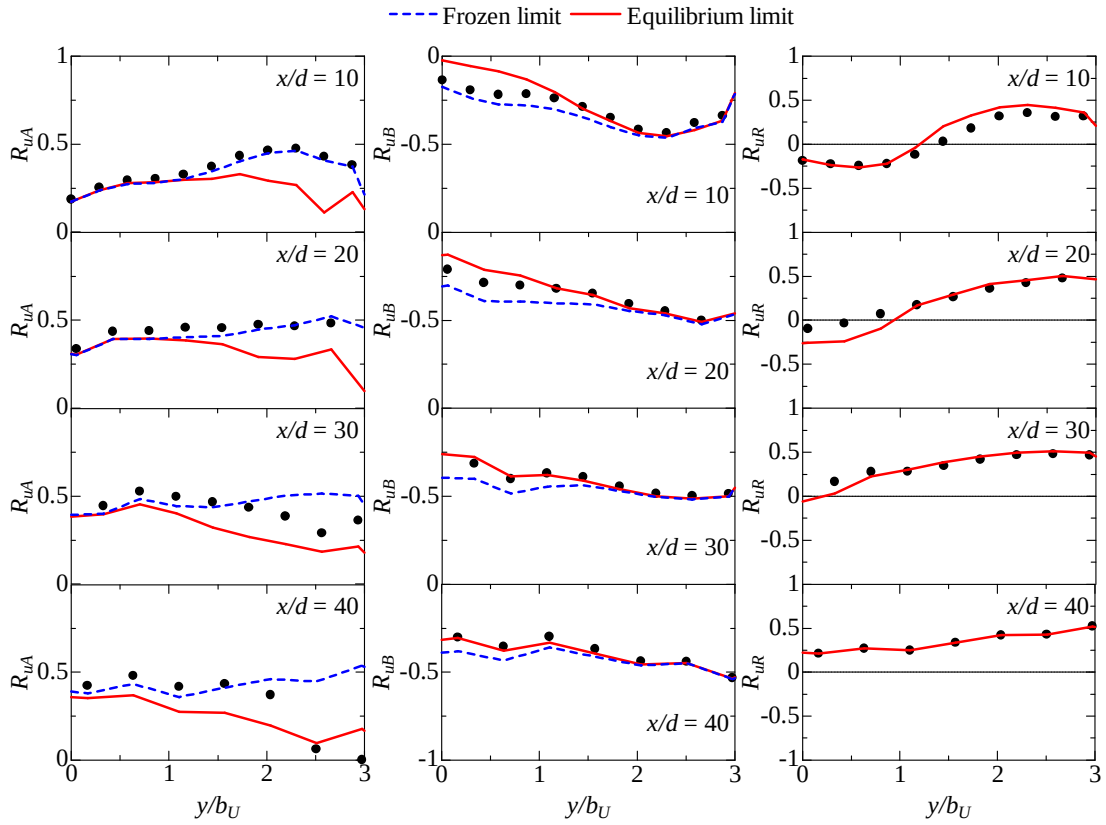

Figure 6. The lateral profiles of the correlation coefficients of the velocity fluctuation and the concentration fluctuation.

4. Results

4.1. Correlation Coefficient

Figures 5 and 6 show the streamwise evolution and the lateral profiles of the correlation coefficients R_{ui} between the streamwise velocity fluctuation u and the concentration fluctuation γ_i (i = A, B or R), respectively. Figures 5 and 6 also show R_{ui} for the frozen

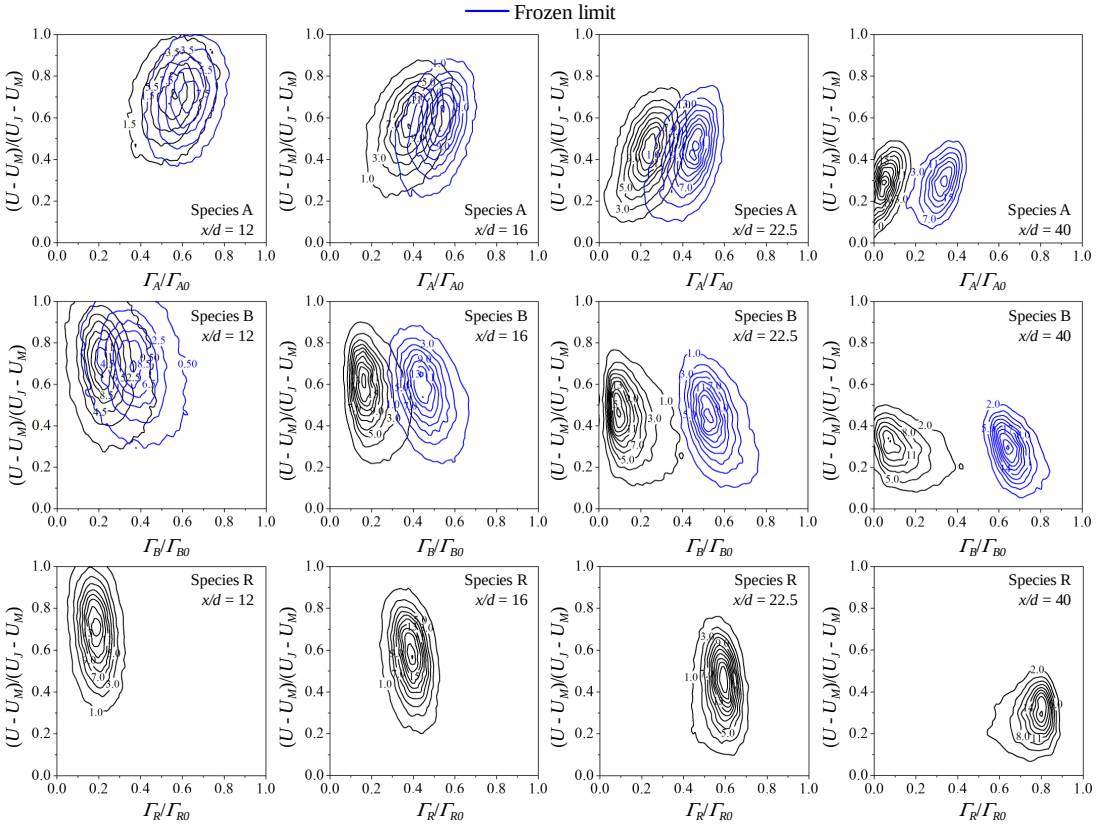

Figure 7. Joint probability density functions of the streamwise velocity and the concentration of reactive species on the jet centreline.

limit and the equilibrium limit. In Fig. 6, the abscissa is normalized by the half-width of the mean velocity profile b_U. Figure 5 shows that R_{uA} is close to that for the frozen limit in the upstream region because the chemical reaction scarcely proceeds whereas R_{uA} becomes large in the downstream region owing to the progress of the chemical reaction. From Fig. 6, it is found that R_{uA} is smaller than that for the frozen limit near the outer edge of the jet at $x/d = 30$ and 40, and R_{uA} for the equilibrium limit is also smaller than that for the frozen limit in the downstream region. These results imply that R_{uA} becomes smaller than that for the frozen limit in the region where most of species A is consumed by the chemical reaction. For species B, Figs. 5 and 6 show that the chemical reaction makes the absolute value of R_{uB} small. Near the outer edge of the jet where the concentration of another reactant species A is very small, R_{uB} is nearly equal to that for the frozen limit whereas the influence of the chemical reaction on R_{uB} is large near the jet centreline where most of species B is consumed by the chemical reaction. These results show that the correlation coefficient between u and γ_i is strongly influenced by the chemical reaction in the region where the concentration of the reactant is small. This is because the chemical reaction consumes most amount of the reactant in those regions. Figures 5 and 6 show that R_{uR} has a negative value

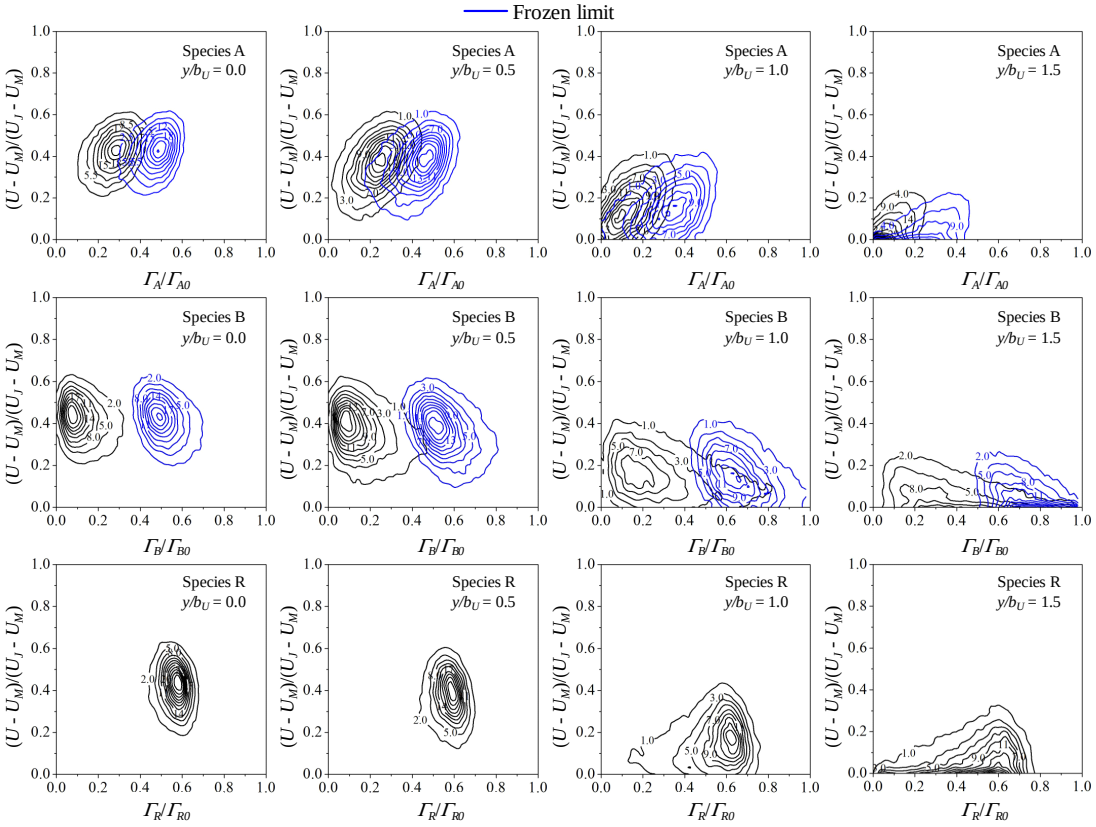

Figure 8. Joint probability density functions of the streamwise velocity and the concentration of reactive species at $x/d = 20$.

in the upstream region and near the jet centreline at $x/d = 10$ and 20 whereas it has a positive value in the downstream region and near the outer edge of the jet. This tendency is explained on the basis of the mass conservation law given by Eq. (8) and the dependency of the reaction rate on the concentrations of reactant species[16].

4.2. Joint Probability Density Function

Figure 7 shows the joint probability density functions (JPDFs) of the streamwise velocity $(U - U_M)$ and the concentration of reactive species, Γ_i (i = A, B or R), on the jet centreline, and Fig. 8 shows the JPDF of $(U - U_M)$ and Γ_i across the jet at $x/d = 20$. In Figs. 7 and 8, $(U - U_M)$ is normalized by the relative mean velocity at the jet exit $(U_J - U_M)$ and Γ_i is normalized by Γ_{i0}. In Figs. 7 and 8, the frozen limit is also shown, but the equilibrium limit is not shown here since the JPDF of the velocity and the reactant concentration for the equilibrium limit has a strong peak near $\Gamma_i \simeq 0$. From Fig. 7, it is found that the JPDF for the reacting case is similar to that for the frozen limit in the upstream region $(x/d = 12)$ where the chemical reaction scarcely proceeds, and the chemical reaction makes Γ_A and Γ_B small by consuming the reactant species A and B in the downstream region. Near the outer edge of the jet, the concentration

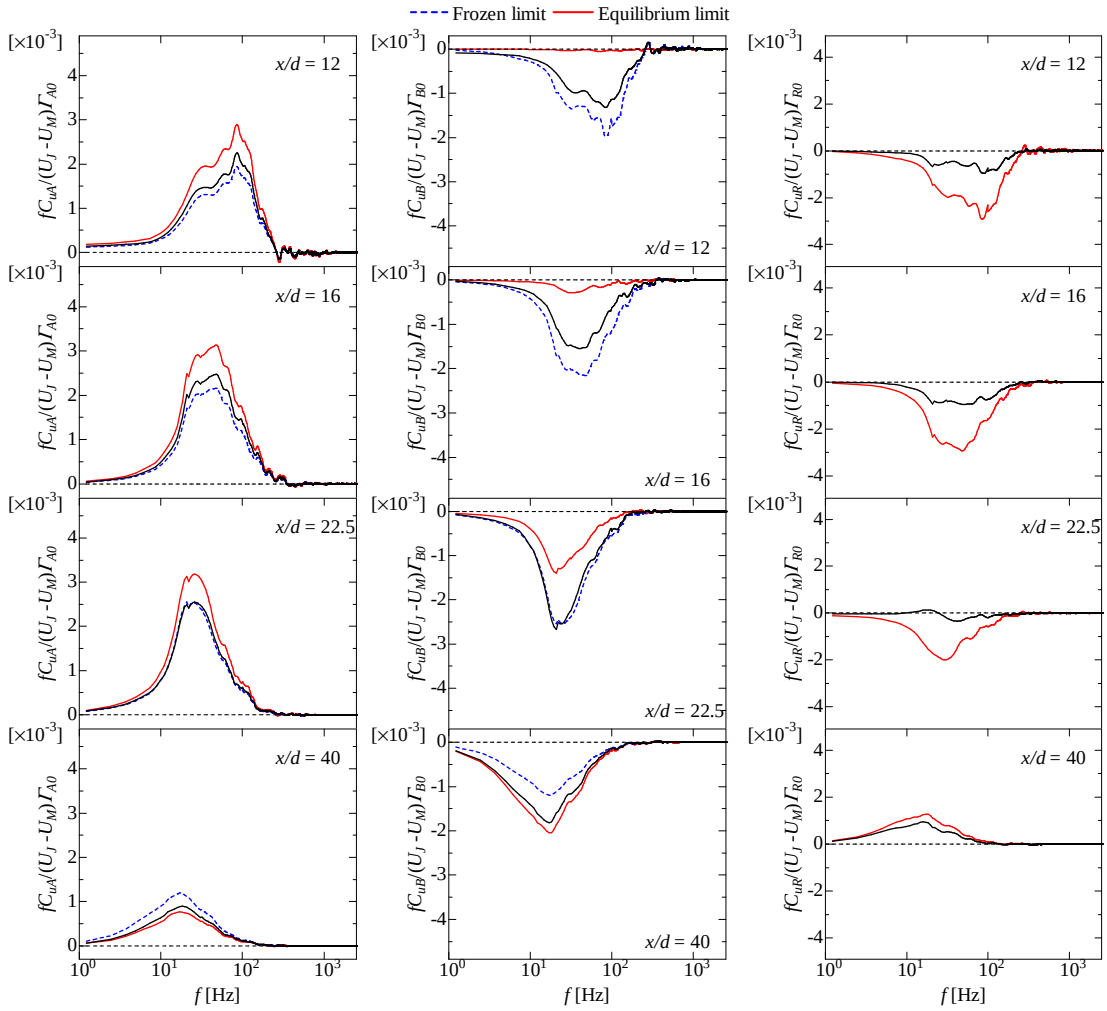

Figure 9. Cospectra of the velocity fluctuation and the concentration fluctuation on the jet centreline.

of species B for the frozen limit, $\tilde{\Gamma}_B^0$, may be nearly equal to Γ_{B0}. If $\tilde{\Gamma}_B^0 \simeq \Gamma_{B0}$, the chemical reaction rate is very small since another reactant species A does not almost exist at the measuring point. The JPDF of $(U-U_M)$ and Γ_B maps over a broader range $0 \leq \Gamma_B \leq \Gamma_{B0}$ than that for the frozen limit because the reactant species B is consumed by the chemical reaction.

Figure 7 also shows that the JPDF of $(U-U_M)$ and Γ_R maps to small Γ_R and large $(U-U_M)$ in the upstream region where the product concentration is small. In contrast, it maps to large Γ_R and small $(U-U_M)$ in the downstream region. Figure 8 shows that the JPDF of $(U-U_M)$ and Γ_R maps over the broad range $0 \leq \Gamma_R \leq \Gamma_{R0}$ near the outer edge of the jet as for that of $(U-U_M)$ and Γ_B.

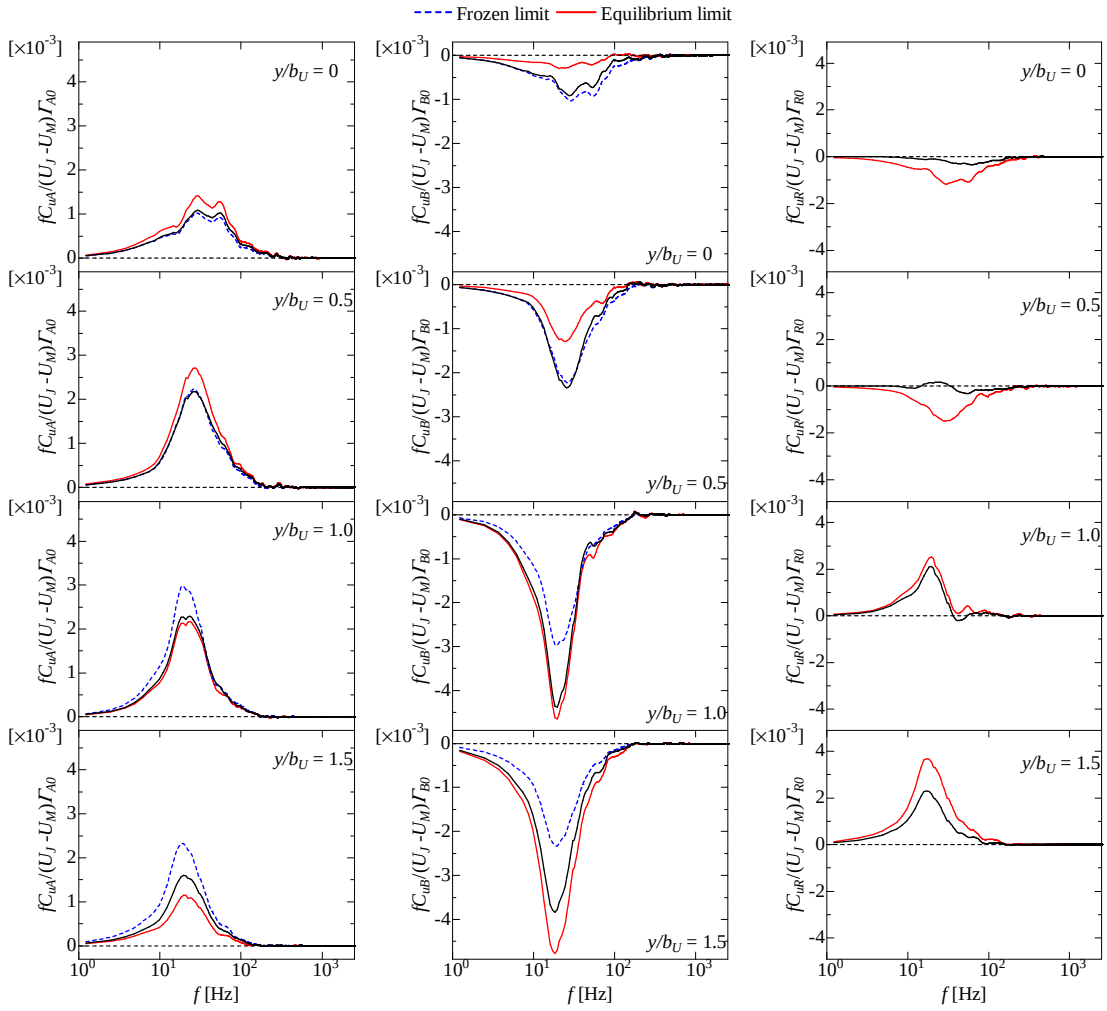

Figure 10. Cospectra of the velocity fluctuation and the concentration fluctuation at $x/d = 20$.

4.3. Cospectra

Figure 9 shows the cospectra C_{ui} (i = A, B, or R) of the streamwise velocity fluctuation u and the concentration fluctuation γ_i on the jet centreline, and Fig. 10 shows C_{ui} across the jet at $x/d = 20$. In Figs. 9 and 10, C_{ui} is normalized by $(U_J - U_M)$ and Γ_{i0}. Figures 9 and 10 also show the cospectra of u and γ_i for the frozen limit and the equilibrium limit. Figures 9 and 10 show that C_{uA} is larger than that for frozen limit in the upstream region and near the jet centreline whereas C_{uA} is smaller than that for the frozen limit in the downstream region and outer edge of the flow. It is also shown that C_{uB} has the negative value, and the magnitude of C_{uB} is smaller than that for the frozen limit in the upstream region and near the jet centreline whereas it is larger than that for the frozen limit in the downstream region and the outer edge of the flow. C_{uR} has a negative value in the upstream region and near jet centreline and become close to 0 as moving in x and y direction. In further downstream region and the outer edge of

the flow, C_{uR} has a positive value.

5. Conclusions

Simultaneous measurements of streamwise velocity and concentrations of reactive species are conducted in a planar liquid jet with a second-order chemical reaction (A + B → R) to investigate the joint statistics between the streamwise velocity and the concentrations of reactive species. The main results are summarized as follows:

(i) The correlation coefficient R_{uA} of the streamwise velocity fluctuation and the concentration fluctuation of reactant species A is smaller than that for the frozen limit near the outer edge of the jet at $x/d = 30$ and 40, whereas it is larger than that for the frozen limit in the upstream region and near the jet centreline at $x/d = 30$ and 40. However, the absolute value of the correlation coefficient R_{uB} of the streamwise velocity fluctuation and the concentration fluctuation of reactant species B becomes small owing to the chemical reaction. The correlation coefficient R_{uR} of the streamwise velocity fluctuation and the concentration fluctuation of product species R has a negative value in the upstream region whereas it has a positive value in the downstream region and near the outer edge of the jet.

(ii) The joint probability density functions of the streamwise velocity and reactant concentration are nearly unchanged by the chemical reaction in the upstream region. In the downstream region, the concentrations of reactants become smaller than that for the frozen limit since the chemical reaction consumes the reactants. The JPDFs of the streamwise velocity and the concentration of species B and R in a reacting case map over the broad range $0 \leq \Gamma_B \leq \Gamma_{B0}$ and $0 \leq \Gamma_R \leq \Gamma_{R0}$, respectively.

(iii) C_{uA} is larger than that for frozen limit in the upstream region and near the jet centreline whereas it is smaller than that for frozen limit in the downstream region and the outer edge of the flow, where C_{ui} (i = A, B or R) is the cospectra of the streamwise velocity fluctuation and the concentration fluctuation of species i. By contrast, the magnitude of C_{uB} is smaller than that for the frozen limit in the upstream region and near the jet centreline whereas it is larger than that for the frozen limit in the downstream region and the outer edge of the flow. C_{uR} has a negative value in the upstream region and near the jet centreline and has a positive value in the downstream region and the outer edge of the flow.

Acknowledgments

The authors would like to thank Dr. Takashi Kubo and Mr. Hiroki Yasuhara for their help in this study. This work was supported by Grants-in-Aid for Scientific Research Nos. 22360077, 23656133 and 23656134.

References

[1] Fox RO 2003 *Computational Models for Turbulent Reacting Flows* (Cambridge: Cambridge University Press)
[2] Veynante D and Vervisch L 2002 *Prog. Energy Combust. Sci.* **28** 193–266
[3] Bilger RW, Saetran LR and Krishnamoorthy LV 1991 *J. Fluid Mech.* **233** 211–242
[4] Brown RJ and Bilger RW 1996 *J. Fluid Mech.* **312** 373–407
[5] Li JD and Bilger RW 1996 *J. Fluid Mech.* **318** 339–372
[6] Bennani A and Gence JN and Mathieu J 1985 *AIChE J.* **31** 1157–1166
[7] Mehta RV and Tarbell JM 1987 *AIChE J.* **33** 1089–1101
[8] Komori S, Kanzaki T and Murakami Y 1991 *Phys. Fluids* **3** 507–510
[9] Kubo T, Sakai Y, Nagata K and Iida K 2009 *JFST* **4** 368–378
[10] Zhdanov V and Chorny A 2011 *J. Heat Mass Transfer* **54** 3245–3255
[11] Komori S, Nagata K, Kanzaki T and Murakami Y 1993 *AIChE J.* **39** 1611–1620
[12] Lee J and Brodkey RS 1964 *AIChE J.* **10** 187–193
[13] Nakamura I, Sakai Y and Miyata M 1987 *J. Fluid Mech.* **178** 379–403
[14] Bourne JR, Hilber C and Tovstiga G 1985 *Chem. Engng Commun.* **37** 293–314
[15] Sakai Y, Nakamura I and Kubo T 1997 *Proc. 11th Symp. on Turbulent Shear Flows* **2** 19–24
[16] Watanabe T, Sakai Y, Nagata K, Terashima O and Kubo T 2011 *Exp. Fluids* submitted